Electrodisintegration of Cu^{63} and Mn^{55}†*

R. L. HINES‡
University of Michigan, Ann Arbor, Michigan

(Received June 18, 1956; revised manuscript received December 7, 1956)

The electrodisintegration of Cu^{63} and Mn^{55} has been investigated for total electron energies from 29.5 Mev to 81.5 Mev by a stacked-foil experiment using the internal electron beam of a synchrotron. The value of $\bar{F}$, which is essentially the ratio of photon induced foil activity to electron induced foil activity, is found to be 8.32 ± 0.54 at 29.5 Mev, 5.47 ± 0.36 at 46.5 Mev, 5.31 ± 0.25 at 63.5 Mev, and 4.97 ± 0.05 at 81.5 Mev for the $Cu^{63}(e,e'n)Cu^{62}$ reaction. For the $Mn^{55}(e,e'3n)Mn^{52*}$ reaction, which has an effective excitation energy of 42 Mev, $\bar{F}$ is found to be 6.67 ± 0.41 at 63.5 Mev and 7.43 ± 0.40 at 81.5 Mev. Upon comparing these values with the theoretical values of $\bar{F}$ for different multipole photon absorption processes, it appears that the resonance peak in the nuclear photon absorption cross section for copper is due to a mixture of 97% of an electric dipole process and 3% of an electric quadrupole process. Nuclear size effects might make the experimental results compatible with a larger proportion of electric quadrupole process. Above the resonance peak, at energies near 42 Mev, the photon absorption appears to be due to either an electric dipole or a magnetic dipole process, but not an electric quadrupole process.

INTRODUCTION

THE electrodisintegration of nuclei is closely related to the more widely investigated process of nuclear photodisintegration. In both cases the nucleus receives its excitation energy through the interaction of an electromagnetic field with the nuclear charge density. In fact, in the theoretical calculation of the cross sections, the matrix element involving the nuclear wave functions is the same. When one forms the ratio of the two cross sections, the unknown nuclear matrix element cancels out leaving a quantity which is dependent on the multipole order of the photon absorption process, and which can be determined experimentally. Comparison of these experimental and theoretical values gives information on the multipole order of the photon absorption process.

An extensive investigation of electrodisintegration of Cu^{63}, Zn^{64}, Ag^{109}, and Ta^{181} at energies from 24 to 35 Mev has been reported by Brown and Wilson,[1] hereafter referred to as BW, who also discuss the earlier work. Additional measurements on Cu^{63} from 14 to 20 Mev are given by Scott, Hanson, and Kerst.[2] BW conclude that the photon absorption process is a mixture of 88% of electric dipole and 12% of electric quadrupole. In this paper, experimental results are presented for $Cu^{63}(e,e'n)Cu^{62}$ from 29.5 to 81.5 Mev and also for $Mn^{55}(e,e'3n)Mn^{52*}$ at 63.5 and 81.5 Mev. The higher energy gives a more sensitive determination of the amount of electric quadrupole excitation. The data for Mn^{55} give information on the multipole order of the photon absorption process for high photon energies.

The general features of the nuclear photon absorption cross section are known from photodisintegration experiments. The cross section rises to a pronounced resonance type peak at about 20 Mev and then falls to a relatively low value above 30 Mev. The actual magnitude and location in energy of the peak are slowly varying functions of the atomic number of the nucleus. An approximate picture of the photon absorption cross section can be obtained from the neutron yield cross section given by Jones and Terwilliger[3] (Fig. 1). The two cross sections differ by a factor due to the competing process of proton emission and the multiplicity of neutron emission at higher energies. The $Cu^{63}(\gamma,n)Cu^{62}$ cross section given by Katz and Cameron[4] is shown to illustrate that this reaction is due to photon energies in the region of the resonance peak. The cross section for the $Mn^{55}(\gamma,3n)Mn^{52*}$ reaction given by Hines[5] is also shown to illustrate that it is due to photon energies which lie above the resonance peak. Manganese and copper are close enough in atomic number to insure that differences in their photon absorption cross sections are small.

The ratio of photodisintegration excitation to electrodisintegration cross section is determined by a stacked-foil experiment. The electron beam impinges on a stack of thin foils having a total thickness approximately 1/30 of a radiation length. When the resultant radioactivity of the foils is plotted as a function of the position of the foil in the stack, a straight line is obtained. The ratio of the slope to the intercept is the desired experimental quantity. The experimental arrangement reported here differs from that used by previous investigators in that an internal synchrotron beam is used as an electron source. It is shown that the photon background is small, and the effect of electrons scattering out of the edge of the target is also small.

† This research was supported by the U. S. Atomic Energy Commission.

* This work is based on a thesis submitted to the Department of Physics, University of Michigan, October, 1953, in partial fulfillment of the requirements for the degree of Doctor of Philosophy.

‡ U. S. Atomic Energy Commission Predoctoral Fellow, now at the Scientific Laboratory, Ford Motor Company, Dearborn, Michigan.

[1] K. L. Brown and R. Wilson, Phys. Rev. **93**, 443 (1954).

[2] Scott, Hanson, and Kerst, Phys. Rev. **100**, 209 (1955).

[3] L. W. Jones and K. M. Terwilliger, Phys. Rev. **91**, 699 (1953).

[4] L. Katz and A. G. W. Cameron, Can. J. Phys. **29**, 518 (1951).

[5] R. L. Hines, Phys. Rev. **91**, 474(A), (1953), and Ph.D. dissertation, Physics Department, University of Michigan, 1953 (unpublished).

THEORY

The theoretical cross section for disintegration of nuclei by electrons has been calculated by Wick,[6] Blair,[7] and Thie, Mullin, and Guth.[8] In addition, BW discuss the theory and emphasize the nature of the approximations involved. The essential point is that the electrodisintegration cross section, $\sigma^{el}(k,E_0)$, for the excitation of a nucleus by a quantum of energy k from an electron of total energy E_0, bears a simple relationship to the photodisintegration cross section, $\sigma^{\gamma}(k)$, of the same nucleus. It is shown that

$$\sigma^{el}(k,E_0)=N_l(k,E_0)\sigma^{\gamma}(k), \tag{1}$$

where l is the multipole order of the photon absorption process. The quantity $N_l(k,E_0)$, which is given explicitly elsewhere,[8] can be thought of as a virtual spectrum of photons which is equivalent to an electron as in the Weizsäcker-Williams approximation.[9] Two important approximations are made in the theoretical calculation. The nucleus is assumed to be a point charge, and plane waves are used for the wave functions of the incident and outgoing electrons.

When a stack of target foils is bombarded by an electron beam, the measured activity u per unit foil thickness at a depth of t g/cm^2 in the target is

$$u=C(1+\bar{F}_l t/g), \tag{2}$$

where $g=A/[Z(Z+1)r_0^2N_0]$. Z and A are respectively the atomic number and weight of the target, $r_0=e^2/\mu$ is the classical electron radius, e is the electronic charge, μ is the rest energy of the electron, and N_0 is Avogadro's number. The proportionality factor C depends on electron beam intensity, counting efficiency, decay half-life, and electrodisintegration cross section, but it is a constant for a given target stack. The quantity of interest is

$$\bar{F}_l=\frac{1}{Z(Z+1)r_0^2}\int_0^{E_0-\mu}\phi\sigma^{\gamma}dk\Big/\int_0^{E_0-\mu}N_l\sigma^{\gamma}dk, \tag{3}$$

where ϕ is the Bethe-Heitler[10] bremsstrahlung cross section for the extreme relativistic case including screening. The use of $Z(Z+1)$ in place of Z^2 takes into account the contribution of the orbital electrons. $\bar{F}$ is experimentally determined by fitting Eq. (2) to the plot of foil counting rates *vs* the depth of the center of the foils in the target stack. A slight variation in the procedure, which is employed by BW, is to measure the activities w_1 and w_2 of two foils of thicknesses x_1 and x_2 separated by a radiator of thickness x_r. By generalizing Eq. (2) to include a radiator of different Z from the target foils, it follows that

$$\bar{F}=\left[\frac{(x_1/x_2)w_2-w_1}{w_1-k_z w_2}\right]\frac{g_r}{t_{\text{eff}}}, \tag{4}$$

where $k_z=(hx_1^2)/2x_2t_{\text{eff}}$, $h\simeq Z(Z+1)A_r/AZ_r(Z_r+1)$, and $t_{\text{eff}}=x_r+[x_1+x_2/2]h$. The subscript r refers to the radiator.

The effect of mixtures of electric dipole and electric quadrupole interactions is readily evaluated by substituting $\sigma^{\gamma}=\sigma_{1e}{}^{\gamma}+\sigma_{2e}{}^{\gamma}$ in Eq. (3) which gives

$$\bar{F}=(1+f)/[(1/\bar{F}_{1e})+(f/\bar{F}_{2e})], \tag{5}$$

where

$$f\simeq\int_0^{E_0-\mu}\sigma_{2e}{}^{\gamma}dk\Big/\int_0^{E_0-\mu}\sigma_{1e}{}^{\gamma}dk.$$

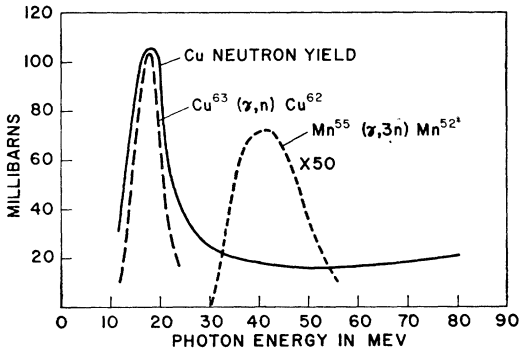

FIG. 1. Photoneutron yield cross section for Cu shown in comparison with $Cu^{63}(\gamma,n)Cu^{62}$ and $Mn^{55}(\gamma,3n)Mn^{52*}$ cross sections.

EXPERIMENTAL APPARATUS AND PROCEDURE

The stack of target foils is bombarded by the internal electron beam of the University of Michigan synchrotron. The target stack is clamped in a holder located on the inside of the equilibrium orbit in one of the zero magnetic field sectors of the machine. When the electron beam reaches the desired energy, the accelerating oscillator is turned off. As the magnetic field continues to increase, the orbit of the electron beam contracts until the beam strikes the target stack. Figure 2 shows the spatial relationship between the electron beam, the target stack, and the target holder. The target holder is made as light as possible to minimize photon production by the few electrons which strike the holder. An air lock is used to insert and remove the target stack and holder from the synchrotron vacuum system.

Figures 3 and 4 show, respectively, the r and z profiles of the activity induced in a copper target by an 80-Mev electron beam. The dotted line gives the activity in a 5-mil foil at the front of a target 138 mils thick, and the solid line gives the activity in a 5-mil foil at the back of the target. These profiles are determined by slicing the activated foils into sections and counting the activity of each section. The activity of

[6] G. C. Wick, Ricerca sci. **11**, 49 (1940).
[7] J. S. Blair, Phys. Rev. **75**, 907 (1949); and "Summary of Calculations on Electron Disintegration of Nuclei," Department of Physics, University of Illinois, 1948 (unpublished).
[8] Thie, Mullin, and Guth, Phys. Rev. **87**, 962 (1952).
[9] W. Heitler, *The Quantum Theory of Radiation* (Oxford University Press, Oxford, 1949), second edition, p. 263.
[10] H. Bethe and W. Heitler, Proc. Roy. Soc. (London) **A146**, 93 (1934).

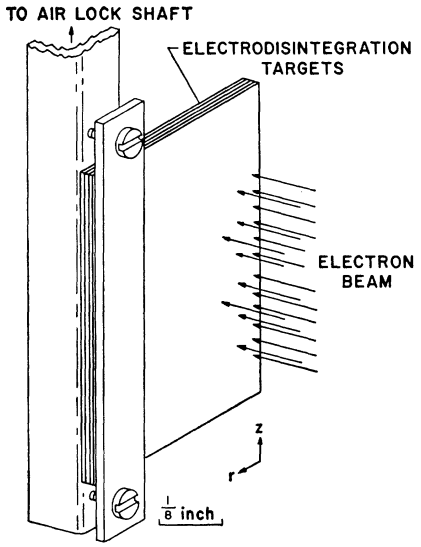

FIG. 2. Spatial relationship of target foils, target holder, and electron beam.

each section at the end of bombardment is computed using a 10.1-minute half-life for the Cu^{62} activity after a correction has been made for counter background and activity of long half-life. The sections are weighed to accurately determine the activity per unit area. The profiles are approximately the same for very thin targets. At 30 Mev the r profile is approximately the same, but the z profile is somewhat wider. The r profile at both 30 and 80 Mev is considerably wider than that predicted by Camac.[11] The discrepancy is probably due

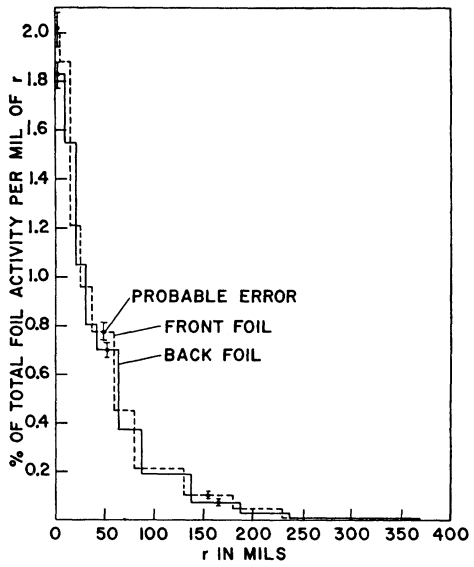

FIG. 3. Profile in r of the induced activity at the front and back of a copper target at 81.5 Mev. Zero point in r is the target edge struck by the electron beam.

[11] M. Camac, Rev. Sci. Instr. 24, 290 (1953).

to the location of the target in a field-free region instead of the ideal synchrotron guide field postulated by Camac.

The target stack for the determination of $\bar{F}$ for Cu^{63} consists of four copper foils 0.7 in. by 0.3 in. with an approximate thickness of 0.10 g/cm^2. The targets are formed by clamping a stack of foils between brass blocks and milling off all four edges to insure that the targets have square edges and are the same size. The thickness of each foil in g/cm^2 is determined from its weight and its length and width as measured with a micrometer. The manganese target stack consists of two manganese foils 0.7 in. by 0.3 in. with an approximate thickness of 0.080 g/cm^2 separated by a copper radiator 0.7 in. by 0.3 in. and 0.798 g/cm^2 thick. The manganese foils are formed from high-purity manganese powder held together by 1% by weight of collodion binder. The C^{11} activity from this amount of collodion is experimentally determined to be 10% of the Mn^{52*} activity. From the activities produced when the two foils are bombarded by a photon beam, it is calculated that the ratio of the two thicknesses is 1.06 ± 0.05. The two manganese foils are interchanged on half of the bombardments to average out thickness differences. Both target stacks are assembled in a jig so that the edges of the individual foils are flush. When the target stack is inserted in the synchrotron, the edge of the stack is aligned parallel to the equilibrium orbit of the electron beam.

The energy of the electron beam is calculated from the equilibrium orbit radius and the magnetic field at turnoff of the accelerating oscillator. The magnetic field is determined by the measured peak magnetic field and the turnoff time of the oscillator. The equilibrium orbit radius is determined by the measured frequency of the accelerating oscillator and the length of the zero magnetic field sectors. The relative values of energy are accurate to $\pm1\%$ and the absolute accuracy of the energy calibration is $\pm5\%$.

The target stacks are bombarded for a time equal to twice the half life of the desired activity. A few minutes after bombardment, the foil activities are counted with a thin wall aluminum Geiger counter (Victoreen 1B85). For a given run, all of the foils are counted with the same counter to eliminate corrections for counter efficiency. A holder is used to maintain the target foils in a fixed position relative to the counter. Experiments with a Cs^{137} source, having the same spatial distribution of activity as the targets, show that the uncertainty in counting rate due to variations in source position is $\pm1\%$. The observed counting rates are corrected for counter background and activity of long half-life. The foil activities range from 400 to 2000 counts/min for the copper foils and from 10 to 60 counts/min for the manganese foils. The foil activities at the end of bombardment are computed using a 10.1-minute half-life for Cu^{62} and a 21-minute half-life for Mn^{52*}.

TABLE I. Summary of experimental results and corrections.

Reaction	E_0 (Mev)	$\bar{F}_{\text{apparent}}$	Edge scattering	Photon degradation	Electron degradation	Total correction	$\bar{F}_{\text{corrected}}$
$Cu^{63}(e,e'n)Cu^{62}$	29.5	7.51±0.49	1.0195	1.048	1.037	1.108	8.32±0.54
	46.5	5.13±0.34	1.0132	1.024	1.028	1.067	5.47±0.36
	63.5	5.04±0.24	1.0095	1.020	1.023	1.053	5.31±0.25
	81.5	4.76±0.05	1.0064	1.017	1.020	1.044	4.97±0.05
$Mn^{55}(e,e'3n)Mn^{52*}$	63.5	5.98±0.37	1.0224	1.067	1.022	1.115	6.67±0.41
	81.5	6.83±0.36	1.0173	1.051	1.018	1.088	7.43±0.40

RESULTS AND DISCUSSION

The experimental results and corrections are summarized in Table I. For copper, the value of $\bar{F}$ is obtained by fitting the straight line given by Eq. (2) to the foil counting rates per unit thickness using the method of least squares. The value given at each energy is the arithmetic mean of five measurements of approximately equal weight. The probable error is calculated from the deviations of the individual measurements from the mean. The probable errors expected from counting rates are the same as those based on the deviations from the mean. This shows that the expected deviation in counting rates is the only important source of statistical error. The value of $\bar{F}$ for manganese is calculated from the counting rates of the two foils using Eq. (4). The value at each energy is the weighted average of four measurements. The weight of each measurement is determined by the number of observed counts. As before, the probable error is calculated from the deviations of the individual measurements from the mean.

There are several corrections which must be made before the experimental results are compared with the theoretical values of $\bar{F}$. If a photon background induces an activity equal to ϵ times the electron induced activity, then the correction factor for photon background can be determined from Eq. (2) to be

$$\bar{F}_{\text{corrected}}/\bar{F}_{\text{apparent}}=1+\epsilon. \tag{6}$$

Since the target dimensions are small compared with the distance to surrounding objects, the photon background is expected to be uniform over the target. The electron flux, however, is concentrated near the edge. Thus a photon background decreases the ratio of activities of a foil in the back of the stack to that in front of the stack most for regions where the electron flux is low. Quantitative comparison of the two graphs given in Fig. 3 gives $\epsilon=0.006\pm0.006$ at a total electron energy of 81.5 Mev. This is of the order of, or less than, the statistical error in $\bar{F}$ so no correction is made.

As the electrons pass through the stack they undergo multiple scattering. Consequently, some will be scattered out through the edge of the target. Likewise, some of the photons created near the edge of the target will pass out through the edge before traversing the entire stack. From the theory of multiple scattering,[12] it can be shown that the fractions δ_{el} and δ_γ of the electron and photon beams respectively which have been scattered out of the edge of the stack at a depth t are given by

$$\delta_{el}=0.20D(0)\theta_s t^{\frac{3}{2}}, \tag{7}$$

$$\delta_\gamma=0.18D(0)\theta_s t^{\frac{3}{2}}, \tag{8}$$

where

$$\theta_s=E_s/(E_0X_0^{\frac{1}{2}}),$$

X_0 is the radiation length of the target material, $E_s=21$ Mev, and $D(0)$ is the distribution function of the electron beam as given in Fig. 3 evaluated at $r=0$. The factor required to correct for edge scattering when Eq. (2) is used to evaluate $\bar{F}$ is given in Table I.

The various assumptions made in the derivation of Eq. (2) are discussed in detail by BW. They give explicit expressions for the changes in the photon spectrum and the virtual spectrum of the electron which arise from electron energy degradation and photon absorption in a target of finite thickness. The correction factors for these effects are given in Table I and are calculated using the spectra given by BW. The true corrections would be the values averaged over the photon energies for which the excitation cross section is finite. However, for this experiment it is sufficiently accurate to assume an effective excitation energy of 18

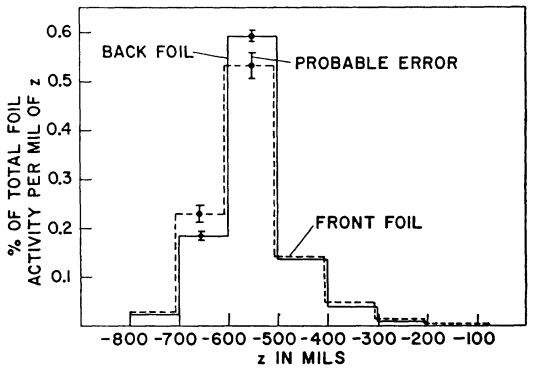

FIG. 4. Profile in z of induced activity at the front and back of a copper target at 81.5 Mev. Zero point in z is the geometric center of the synchrotron doughnut.

[12] B. Rossi, *High-Energy Particles* (Prentice-Hall, Inc., New York, 1952), p. 72.

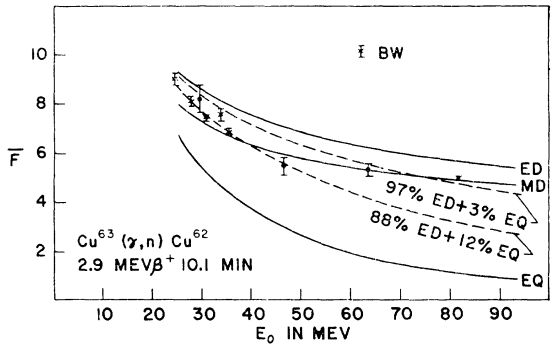

FIG. 5. Experimental and theoretical values of $\bar{F}$ for copper. The dashed lines are computed assuming an effective excitation energy of 14 Mev for the electric quadrupole process.

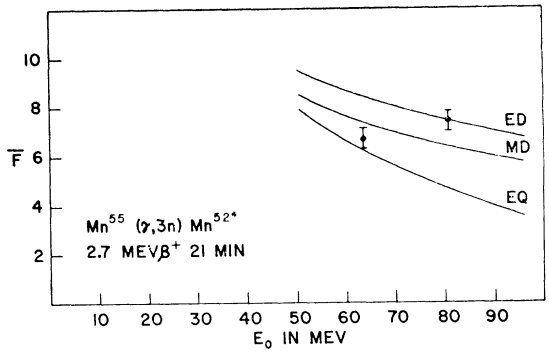

FIG. 6. Experimental and theoretical values of $\bar{F}$ for manganese.

Mev for the Cu^{63} reaction and 42 Mev for the Mn^{55} reaction.

The corrected values of $\bar{F}$ are given in the last column of Table I and are plotted in Figs. 5 and 6. The solid lines in Figs. 5 and 6 are the theoretical values of $\bar{F}$ calculated from Eq. (3) using the cross sections shown in Fig. 1. For comparison, the data of BW are also shown for Cu^{63}. The dotted lines in Fig. 5 are calculated from Eq. (5) using an effective electric quadrupole excitation energy of 14 Mev. The mixture of 88% electric dipole and 12% electric quadrupole, which BW found gave good agreement with their data, does not fit the data given here for higher energies. The fit with the theoretical curve for a magnetic dipole interaction is surprisingly good over the entire energy range. However, a magnetic dipole interaction is eliminated on the grounds that it would give an integrated absorption cross section much smaller than that actually observed. It must be remembered that there is reasonable doubt of the accuracy of the theory at low electron energies owing to the approximation of the electron wave functions by plane waves. Since the approximation should improve as the electron energy increases, the theory should be most accurate at the highest energies. If it is assumed correct in the 60- to 80-Mev range, then it is found that a mixture of only 3% electric quadrupole and 97% electric dipole is required to fit the experimental points. Such a mixture does not fit the low-energy data, but the use of Coulomb wave functions for the electron instead of plane waves might lower the theoretical values of $\bar{F}$. The possible presence of a small amount of magnetic dipole interaction is not considered here. The nearly identical values of $\bar{F}$ for electric dipole and magnetic dipole interactions make the experimental results insensitive in determining mixtures of the two.

For the Mn^{55} reaction, which is due to photon energies beyond the resonance region, the two experimental points shown in Fig. 6 are not sufficient to establish a trend. However, from the results for Cu^{63}, it appears that the theoretical values of $\bar{F}$ are high at electron energies near the nuclear excitation energy. If this hypothesis is used to correct the theoretical values of $\bar{F}$ for Mn^{55}, then the experimental data would fit either the electric dipole or magnetic dipole curve but not the electric quadrupole curve. The magnetic dipole interaction cannot be excluded because the photon absorption cross section at these energies is much smaller than in the giant resonance region.

The effect of finite nuclear size may modify the conclusions concerning the relative amounts of electric dipole (ED) and electric quadrupole (EQ) excitation. The theory assumes that $|\mathbf{K}\cdot\mathbf{R}|$ is small compared to unity, where $\mathbf{K}$ is the momentum transferred to the nucleus and $\mathbf{R}$ is the radius vector of the interacting nucleon. At the electron energies employed here, $|\mathbf{K}\cdot\mathbf{R}|$ may be several times unity for large electron scattering angles. However, such collisions account for only a minor portion of the total cross section. The value of $|\mathbf{K}\cdot\mathbf{R}|$ which is representative of the bulk of the cross section is given by

$$|\mathbf{K}\cdot\mathbf{R}|_{Av}\simeq K_{Av}R_{Av}|\cos\theta|_{Av}=3K_{Av}R_0/2\pi, \qquad (9)$$

where $K_{Av}=\int K(d\sigma^{el}/d\Omega)d\Omega/\sigma^{el}$, $R_0=1.2\times10^{-13}A^{\frac{1}{3}}$, and θ is the angle between $\mathbf{K}$ and $\mathbf{R}$. The differential cross section for electrodisintegration, $d\sigma^{el}/d\Omega$, is given by Thie, Mullin, and Guth.[8] The values of $|\mathbf{K}\cdot\mathbf{R}|_{Av}$ for the cases of interest here are: 0.25 for Cu^{63} ED at $E_0=36$ Mev; 0.32 for Cu^{63} ED at $E_0=77$ Mev; 0.32 for Cu^{63} EQ at $E_0=36$ Mev; 0.74 for Cu^{63} EQ at $E_0=77$ Mev; 0.53 for Mn^{55} ED at $E_0=77$ Mev; and 0.63 for Mn^{55} EQ at $E_0=77$ Mev. For the Cu^{63} ED interaction, $|\mathbf{K}\cdot\mathbf{R}|_{Av}$ is small enough so that the form factor correction for finite nuclear size is expected to be small. However, for the Cu^{63} EQ interaction $|\mathbf{K}\cdot\mathbf{R}|_{Av}$ approaches unity at high electron energies so the form factor correction might appreciably decrease the electric quadrupole cross section. This would make the experimental results compatible with a larger fraction of quadrupole excitation than is indicated above. A detailed treatment of the effect of nuclear size upon the electrodisintegration cross sections is not at present available in the literature, and it would be a theoretical undertaking beyond the scope of this paper.

CONCLUSION

From the experimental data that have been presented here on the ratios of photodisintegration excitation to electrodisintegration cross section for Cu^{63} and Mn^{55}, the following statements can be made about the nuclear photon absorption cross section for elements near copper. The giant resonance peak near 20 Mev appears to be due to an electric dipole process with a mixture of 3% of an electric quadrupole process. Nuclear size effects might make the experimental results compatible with a larger proportion of electric quadrupole process. The high-energy tail of the photon absorption cross section near 42 Mev appears to be due to either an electric dipole or a magnetic dipole process, but does not appear to be due to an electric quadrupole process.

ACKNOWLEDGMENTS

The author is indebted to Dr. K. M. Terwilliger, Dr. L. W. Jones, and Professor K. M. Case for many discussions and suggestions throughout the course of the work, and is particularly indebted to his advisor, Professor H. R. Crane, who originally suggested the problem of electrodisintegration with the internal synchrotron beam. Professor R. W. Pidd and the synchrotron staff obligingly furnished the high-energy electrons.

PHYSICAL REVIEW VOLUME 105, NUMBER 5 MARCH 1, 1957

Half-Lives of Sc^{46}, Co^{60}, Zn^{65}, Ag^{110m}, Cs^{134}, and $Eu^{152,154}$

K. W. GEIGER
Division of Applied Physics, National Research Council, Ottawa, Canada
(Received November 28, 1956)

The half-lives of six gamma-emitting nuclides were determined by comparison with radium standards, using a lead-shielded ionization chamber. The following results were obtained: Sc^{46}: 83.89±0.12 days; Co^{60}: 5.24±0.03 years; Zn^{65}: 243.5±0.8 days; Ag^{110m}: 252.5±1.5 days; Cs^{134}: 2.07±0.02 years; $Eu^{152,154}$: 12.2±0.2 years. The errors quoted are twice the standard deviation calculated from a least-squares analysis.

THE half-lives of radioactive nuclides that emit hard gamma radiation can be determined with considerable accuracy by comparison with radium on a lead-shielded ionization chamber. Because of its long half-life (1600 years), radium provides an almost constant reference intensity, while the use of a detector insensitive to beta and soft gamma radiation eliminates the effects of a large number of possible radioactive impurities. Half-life measurements have been carried out by this method on six gamma-emitting nuclides.

The investigated nuclides were produced by neutron irradiation in the Chalk River NRX-reactor. The initial activities of the samples were between 100 and 300 mC. Details on composition and purity are given in Table I. The gamma radiation was measured with a one-atmosphere, air-filled, parallel-plate ionization chamber[1] made of aluminum and shielded by 0.6 cm of lead. Saturation properties were studied by the two-source method but no effects within the experimental errors of ±0.15% could be found.

Sources were placed in a light-weight V-shaped hod at distances from 20 to 150 cm from the face of the ionization chamber. The ionziation current was measured by a null method using a Lindemann-Ryerson electrometer as an indicator. The ionization produced by the nuclide under investigation was compared with the ionization from a radium standard of such a strength that the ionization ratio was always between 2 and $\frac{1}{2}$. With one radium standard, therefore, the decay could be observed for about two half-lives, after which a standard of about $\frac{1}{4}$ the strength was chosen. For the half-life calculation no attempt has been made to make use of the relative values of the standards, which were known to ±0.15%, as the half-life would be very sensitive to this ratio. Half-lives were calculated separately for each standard. The standard deviation for a ratio determination between nuclide and standard was ±0.25%. Measurements were made in approximately equal intervals of between 0.08 and 0.2 half-lives according to nuclide. A least-squares analysis of the data was carried out which for none of the nuclides showed a significant deviation from a simple exponential decay.

The results, corrected for the decay of radium ($T_{\frac{1}{2}}$=1600 yr), are given in Table I, together with some of the more recent measurements of previous authors. Since the standards contained only a commercial grade of radium salt, they were compared periodically among themselves and with the Canadian primary radium standard.[2] Their values remained constant within the experimental error of ±0.15%. The standard deviations in the half-life figures, as calculated from the least-squares analyses, have been

[1] W. S. Michel, National Research Council of Canada, Ottawa, Report No. 3675, June, 1955 (unpublished).

[2] C. Garrett and K. W. Geiger, Can. J. Phys. 34, 1075 (1956).